1
2

3

4

An experimental census of retrons for DNA production and genome editing

7

8

Authors: Asim G. Khan[1,#], Matías Rojas-Montero[1,#], Alejandro González-Delgado[1,#],

Santiago C. Lopez[1,2], Rebecca F. Fang[1,3], Seth L. Shipman[1,4,5,*]

11

Affiliations:

[1]Gladstone Institute of Data Science and Biotechnology, San Francisco, CA, USA

[2]Graduate Program in Bioengineering, University of California, San Francisco and Berkeley, CA, USA

[3]Graduate Program in Neuroscience, University of California, San Francisco, CA, USA

[4]Department of Bioengineering and Therapeutic Sciences, University of California, San Francisco, CA, USA

[5]Chan Zuckerberg Biohub – San Francisco, San Francisco, CA

20

[#]equal contributions

22

*Correspondence to: seth.shipman@gladstone.ucsf.edu

ABSTRACT

Retrons are bacterial immune systems that use reverse transcribed DNA as a detector of phage infection. They are also increasingly deployed as a component of biotechnology. For genome editing, for instance, retrons are modified so that the reverse transcribed DNA (RT-DNA) encodes an editing donor. Retrons are commonly found in bacterial genomes; thousands of unique retrons have now been predicted bioinformatically. However, only a small number have been characterized experimentally. Here, we add substantially to the corpus of experimentally studied retrons. We synthesized >100 previously untested retrons to identify the natural sequence of RT-DNA they produce, quantify their RT-DNA production, and test the relative efficacy of editing using retron-derived donors to edit bacterial genomes, phage genomes, and human genomes. We add 62 new empirically determined, natural RT-DNAs, which are not predictable from the retron sequence alone. We report a large diversity in RT-DNA production and editing rates across retrons, finding that top performing editors outperform those used in previous studies, and are drawn from a subset of the retron phylogeny.

INTRODUCTION

The signature of a retron – copious single-stranded DNA of a uniform length produced spontaneously by bacteria – was first observed in 1984[1]. Five years later, it was shown that this DNA was the product of an endogenous reverse transcriptase (RT), the first RT discovered in prokaryotes[2]. The template for the reverse transcribed DNA (RT-DNA) of a retron is a short, highly structured RNA, which is produced from the same operon as the retron RT. The RT recognizes this structured, noncoding RNA (ncRNA) and partially reverse transcribes it into RT-DNA, polymerizing from a critical 2' hydroxyl of the ncRNA[3,4]. The result is a transcriptional/reverse-transcriptional cascade that amplifies a single locus in the bacterial genome up to hundreds of copies of RT-DNA per cell[5]. This phenomenon of RT-DNA production was observed from 16 natural retrons over the next thirty years, without any conclusive evidence for a cellular function[6].

More recently, a cellular role for retrons has become clear. Retrons confer phage resistance to bacteria[7-10]. Full mechanistic details are still emerging, but the general model is that retron RT-DNA is a sensor of phage infection. Either directly or indirectly, the phage modifies or degrades the RT-DNA, which releases an accessory retron protein that acts as a cellular toxin to remove the infected cell and spare the bacterial population[8,9,11]. Individual retrons have been shown to confer specific resistance to particular phages[8,12]. This specificity is due, at least in part, to the unique sequence of RT-DNA produced by the retron[8]. More than a thousand retrons have now been identified in genomic and metagenomic databases by homology to known retron RTs[10]. However, the sequence of the ncRNA has remained difficult to identify bioinformatically and the exact RT-DNA produced by each retron is, thus far, impossible to predict.

62   Retrons, like many other bacterial immune systems, have also proven valuable as

63   a component of biotechnology. Specifically, the faithful production of abundant single-

64   stranded DNA in cells by retrons has been used to produce templates for genome

65   engineering, transcriptional receipts for molecular recorders, and transcription factor

66   decoys[13-17]. Yet, to date, these technologies have been built using only a small number

67   of the early-discovered retrons.

68   It is critical that we survey the diversity of retrons, both to inform investigations of

69   bacterial immunity and to improve retron-based technologies. Of the thousand plus

70   retrons identified[10], only eighteen have actually been shown to produce RT-DNA[6,8,9], only

71   one has been used for bacterial recombineering[13,16,18], and only eight have been tested

72   for human genome editing[18-20]. Here, we address the lack of experimental testing across

73   the diversity of predicted retrons by undertaking a census of RT-DNA production and

74   editing in multiple cellular contexts. We provide validation of noncoding RNA sequence

75   and RT-DNA production for retrons across the phylogeny, and report sequences of the

76   unpredictable RT-DNA that are critical to inform new studies of function and technology.

77   We identify the first subsets of retrons that appear to lack RT-DNA production, which will

78   also inform future work in the field. We also find that particular subtypes of retrons produce

79   higher amounts of RT-DNA and better editing performance.

80

81   **RESULTS**

82   In order to expand the corpus of experimentally validated retrons, we synthesized

83   163 never-before-tested retron RTs and ncRNAs distributed across various experiment

84   types to enable quantification of RT-DNA production, as well as editing in bacterial,

85   phage, and human genomes. These retrons were drawn from a set of 1,928 recently

86   published retrons[10] that were bioinformatically predicted based on protein homology to

87   known retron RTs. While the RT component was previously annotated, the ncRNA

88   component of retrons is difficult to predict across diverse retrons. We identified and

89   annotated the cognate ncRNAs of each RT by simulating RNA folding in regions within

90   500bp of the RT and comparing the overall secondary structure to the consensus ncRNA

91   structures. This consists of conserved characteristics such as an inverted repeat (the

92   a1/a2 region of a retron ncRNA) >8bp, a priming guanine near the beginning of the

93   ncRNA, and multiple hairpins in close proximity to a retron RT. Retrons have been

94   recently shown to engage in phage defense that requires one or more additional

95   accessory proteins, multiple of which have been shown to be cellular toxins[8,9,12]. The

96   accessory proteins and phage defense mechanisms are extremely diverse among

97   retrons[10]. For this work, we chose to focus on a census of the core reverse transcription

98   machinery and use in biotechnology and thus excluded accessory genes from our

99   analysis. However, it is important to note that in some cases the retron RT is fused to

100   accessory domains and, in these instances, we did not truncate the protein.

101

102   **RT-DNA production by a diverse set of retrons**

103   For testing RT-DNA production, we synthesized 98 new retron RTs and ncRNAs,

104   and one known standard, retron-Eco1 (ec86). These retrons were chosen to give a broad

105   representation of the RT phylogeny (**Fig 1a**), including retrons from each RT clade (**Fig**

106   **1b**). Retron ncRNAs are frequently found immediately upstream of the retron RT.

107   However, in this natural arrangement, putative ribosomal binding sites can be contained

108   within the ncRNA, which makes standardization impossible. Therefore, we chose to invert

109   the architecture and create operons driven by a T7/lac promoter, followed by a strong

110   RBS, the RT coding region, and finally the ncRNA (**Fig 1c**). In this arrangement, no

111   additional surrounding sequence other than the inverted repeat a1/a2 regions are present

112   with the ncRNA, so in cases where an RT-DNA is produced, we can be sure that we have

113   rigorously identified the ncRNA.
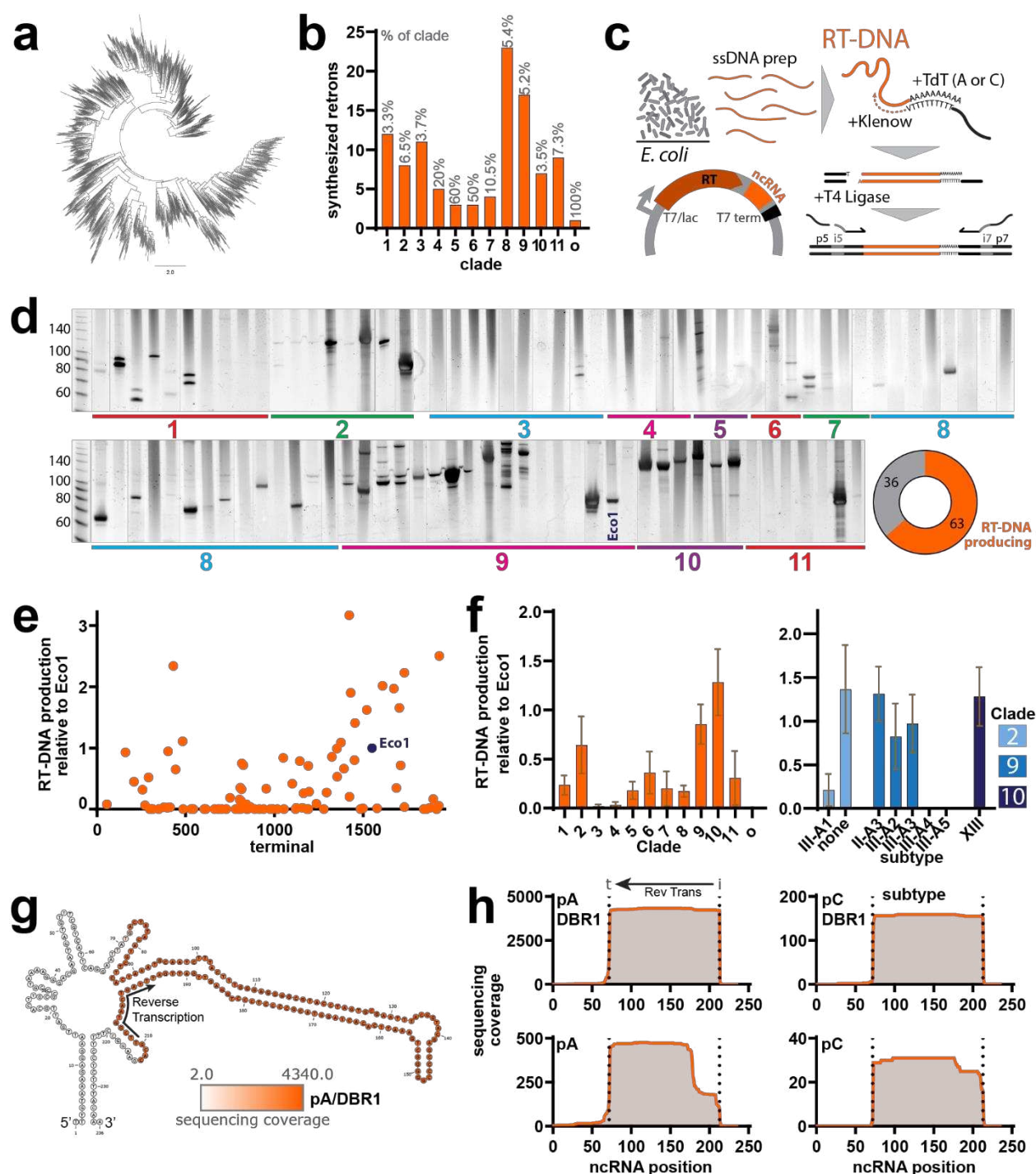
114   We transformed each of these 99 retrons (98 new plus one reference standard)

115   into BL21-AI *E. coli* and induced expression of the synthetic operon for five hours. We

116   prepared non-genomic nucleotides by midiprep and visualized these nucleotides on a

117   TBE/Urea gel to quantify the presence of a characteristic RT-DNA band. Next, we

118   prepared any resulting RT-DNA for sequencing. Because the retron RT-DNA sequences

119   were unknown to us, we adapted an unbiased sequencing approach that we have

120   previously used to examine Eco1 variant libraries[12]. Briefly, we added a single poly-

121   nucleotide handle to the 5' end of RT-DNA using TdT, used a complementary poly-

122   nucleotide anchored primer and Klenow to synthesize a strand complementary to the RT-

123   DNA, and then ligated adapters at the 3' end of the now double-stranded RT-DNA (**Fig

124   1c**). The resulting molecules were indexed and sequenced on an Illumina machine.

125   We found that 62 of the 98 newly tested retrons produced RT-DNA that were

126   detectable on a TBE/Urea gel, which varied in both length and abundance (**Fig 1d**). We

127   quantified the intensity of these bands relative to a standard, retron-Eco1. When these

128   relative production values are plotted by phylogenetic terminal, we observed that retrons

129   in certain regions of the phylogeny produce more RT-DNA than others (**Fig 1e**). When

130   examined by RT clade, we see greatest production from clades 2, 9, and 10; almost no

131   production from clades 3 and 4; and intermediate production from the rest (**Fig 1f**). This

132   can be further broken down by retron subtype – which is based on features of the

133   accessory proteins rather than the RT itself – within the high producing clades. Here, we

134   see that within clades 2 and 9, the highest producing retrons are confined to certain

135   subtypes. This subtype dependence is also evident in some lower producing clades

136   (**Supplementary Fig 1**).

137   We next used the sequencing data to determine the sequence of RT-DNA from

138   retrons that produced it. We aligned RT-DNA sequences determined from the blind prep

139   of single-stranded DNA to each retron ncRNA. An example of sequencing coverage is

140   shown for Mestre-1673, plotting coverage onto the secondary structure of the ncRNA (**Fig**

141   **1g**). Each RT-DNA was prepped in parallel using four similar approaches, varying two

142   parameters. First, we varied the nucleotide that we used to extend the sequence (poly

143   adenine, pA, or poly cytosine, pC) for unbiased sequencing as TdT polymerase has

144   nucleotide preferences that could affect the efficiency of the prep based on the

145   terminating nucleotide of the RT-DNA. Second, we varied whether we pretreated the

146   nucleotides with a debranching enzyme (DBR1) prior to sequencing prep. The

147   characteristic 2'-5' RNA to DNA linkage created when retron RTs polymerize from a

148   structured RNA inhibits our sequencing preparation. For some retrons, this branched

149   molecule is long lasting and DBR1 is required for efficient preparation. However, other

150   retrons are debranched *in vivo* by nucleases that cleave in the RT-DNA. In these cases,

151   DBR1 is not required for efficient sequencing preparation. By including both conditions,

152   we can estimate whether a given retron remains branched or is debranched in vivo.

153   Figure 1h shows each of these four conditions for Mestre-1673, with sequencing

154   coverage plotted over linear ncRNA position. In the pA/DBR1 condition (also shown in

155   Figure 1g), we see even coverage of the RT-DNA region of the ncRNA. We define the

156   initiation point (dashed line i) as the point where coverage increases to ≥15% of maximum

157   coverage and termination (dashed line t) as the point where coverage decreases to ≤50%

158   of maximum coverage. These initiation and termination points are propagated to the other

159   conditions. In this case the pC/DBR1 condition closely matches the pA, but with fewer

160   reads, which is typical of all RT-DNA sequencing. The conditions below, which lack DBR1

161   addition during sequencing prep, have substantially fewer reads. This is consistent with

162   a retron that remains 2'-5' branched *in vivo*. These coverage maps also illustrate a pattern

163   that occurs frequently among retrons. In the absence of DBR1, the 5' end of the RT-DNA

164   begins further from the branched initiation point. This likely represents a fraction of RT-

165   DNA that was debranched *in vivo* by cleavage of the RT-DNA at a position 3' to the branch

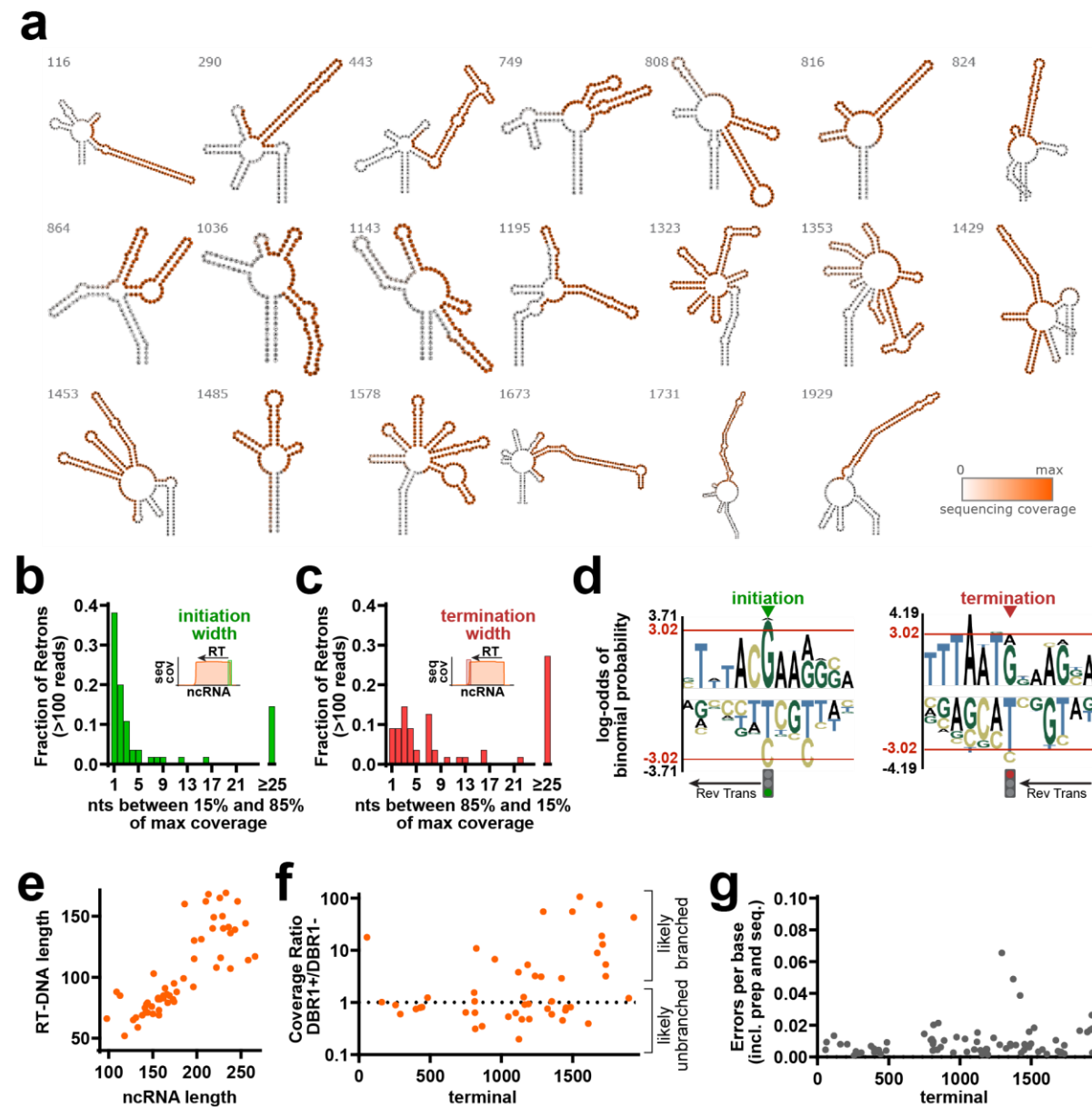166   point or partial nuclease degradation from the free 5' end of a debranched fraction.

167

Figure 1. RT-DNA production by a diverse set of retrons. **a.** Phylogenic analysis of retron RTs[10]. **b.** Number of retrons synthesized by clade (percentage of clade synthesized indicated in gray above each bar). Bar o indicates an orphan, clade-less retron. **c.** Schematic of RT-DNA quantification experiment. Bottom left shows the architecture of retrons for expression, right shows strategy for unbiased sequencing of RT-DNA. **d.** PAGE analysis of all retrons tested (composite of multiple gels, uncropped gels in **Supplemental Figure 6**) and proportion of retrons with detectable RT-DNA (bottom right donut). **e.** Quantification of RT-DNA production by density, relative to retron-Eco1 (marked in blue) arranged by order (terminal number) in the RT phylogeny shown in 1a. **f.** RT-DNA production by clade (one-way ANOVA, effect of clade P=0.0003). Bar o indicates an orphan, clade-less retron. Plot to the right splits production of the top clades by retron subtype. Bars show mean ±SEM. **g.** RT-DNA sequencing coverage plotted onto folded ncRNA for retron Mestre-

177 1673. Orange indicates the bases that are reverse transcribed. **h.** Plots of RT-DNA sequencing coverage by ncRNA
178 position for retron Mestre-1673. Conditions include pA or pC tailing of the RT-DNA for sequencing prep and inclusion
179 or exclusion of DBR1 prior to sequencing prep. Dashed lines indicate the initiation and termination points, defined from
180 the pA/DBR1 condition (initiation: coverage increases to ≥15% of maximum; termination: coverage decreases to ≤50%
181 of maximum). Additional statistical details in **Supplemental Table 2**.
182

183 **Characteristics of RT-DNA production across retrons**

184 　　　We generated RT-DNA coverage maps for 54 retrons. Sequencing coverage (RT-

185 DNA) plotted onto retron ncRNA secondary structures is shown for a subset of retrons in

186 Figure 2a. Coverage and sequencing data for all retrons is provided in accompanying

187 supplemental data (**Supplemental Data 1**). When quantified across retrons, the initiation

188 point is typically quite stringent, with RT-DNA sequencing coverage rising from 15% of

189 maximum to 85% of maximum within 3 nucleotides for >65% of retrons tested (**Fig 2b**).

190 In contrast, termination tended to occur over a wider window, suggesting more variability

191 in the termination point or some degradation of the 3' end after termination (**Fig 2c**). The

192 branching nucleotide of the ncRNA from which the RT-DNA is built has been found to be

193 most frequently a guanine often preceded by TTA, which we also see in our set of

194 functional retrons (**Supplemental Fig 2**). We find that the first reverse transcribed base

195 is also most frequently a guanine and that the termination point of RT-DNA typically

196 precedes an AT rich region of the ncRNA (**Fig 2d**). The length of the ncRNA varies across

197 retrons, and is correlated with the length of the RT-DNA (**Fig 2e**). We can use the ratio of

198 DBR1+ sequencing reads to DBR1- sequencing reads to infer which retrons remain

199 branched *in vivo*. Retrons with similar numbers of reads regardless of the presence or

200 absence of DBR1 in the sequencing prep are likely unbranched already *in vivo*, whereas

201 retrons with many more reads in the DBR1+ condition likely remain branched *in vivo* (**Fig**

202 **2f**). Finally, this RT-DNA sequencing data can be harnessed to estimate the relative

203 fidelity of the retrons by quantifying the errors per base in the RT-DNA with respect to the

204   retron's ncRNA reference. Critically, these are not absolute error rates of the RT as this

205   includes errors introduced by sequencing prep or Illumina sequencing. We find that most

206   retrons are of a similar fidelity, with just a few retrons making ~5x greater errors (**Fig 2g**).

207

Figure 2. Characteristics of RT-DNA production across retrons. **a.** Examples of RT-DNA sequencing coverage plotted on folded ncRNA for a subset of sequenced retrons (additional data in **Supplemental Data 1**). **b.** Strictness of initiation. For all retrons with at least 100 sequencing reads, number of nucleotides at the RT initiation point between 15% an 85% of maximum coverage. **c.** Strictness of termination. For all retrons with at least 100 sequencing reads, number of nucleotides at the RT termination point from 85% to 15% of maximum coverage. **d.** Probability logos showing overrepresented (positive) and underrepresented (negative) nucleotides at the initiation (left) and termination (right)

215   points. Red line indicates $P<0.05$. **e.** RT-DNA length versus ncRNA length (Pearson Correlation, $r^2=0.6586$, $P<0.0001$).
216   **f.** Ratio of the sequencing coverage in the +DBR1 condition versus the –DBR1 condition for each retron. Retrons with
217   a high ratio are more likely to exist in a 2'-5' branched form with their msr, which requires DBR1 for efficient sequencing,
218   whereas retrons with ratios around or under 1 are equally sequenced in the absence or presence of DBR1 indication
219   that they were not 2'-5' branched. **g.** Errors per base versus the ncRNA reference for retrons with at least 1,000
220   sequenced bases, calculated using Levenshtein Distance. Errors include fidelity of the RT, but also errors introduced
221   by the sequencing prep and sequencing. Additional statistical details in **Supplemental Table 2**.
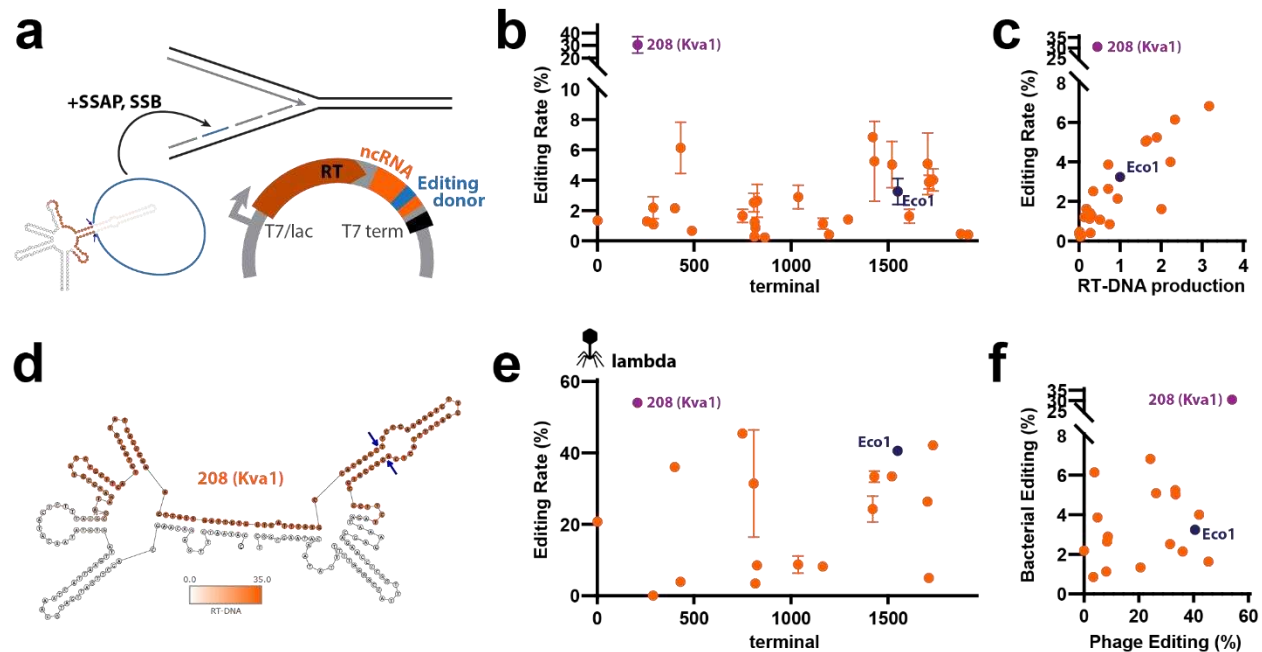
Surveying retrons for bacterial and phage recombineering

223   The ability of retrons to continuously produce a ssDNA containing a precise target

225   mutation has been recently exploited for recombineering purposes in both bacteria and

226   phages[13,16,18,21-23]. Retron-based recombineering relies on the reverse transcription of a

227   modified RT-DNA that contains an editing donor (**Fig 3a**). The host single-stranded

228   binding protein (SSB) will bind the resulting RT-Donor to promote its interaction with a

229   single-stranded annealing protein (SSAP, e.g. CspRecT), which leads to installation of

230   the edit in the lagging strand during chromosome replication[24]. However, only retron-Eco1

231   has been extensively characterized and optimized for use in prokaryotic genome

232   engineering.

233   To survey the ability of retrons to support recombineering, a batch of 29 candidates

234   were selected from our retron library, prioritizing higher RT-DNA producers across the

235   phylogenic tree, and including retron-Eco1 as a reference. The ncRNAs of these retrons

236   were modified to contain a 90 bp template donor to make a precise single nucleotide

237   mutation in *rpoB* gene. The template location was placed within the RT-DNA region as

238   determined by our sequencing data and in a centrally located hairpin stem. After

239   analyzing recombineering efficiencies, we found that 8 retrons yield higher editing rates

240   than retron-Eco1 (**Fig 3b**). We find that RT-DNA production from the wildtype ncRNA and

241   editing using a modified DNA are strongly correlated, consistent with previous work

242   showing that the abundance of recombineering donor is a limiting reagent in editing (**Fig**

243   **3c**). However, the most effective retron for bacterial editing deviates from this correlation.

244   Strikingly, a retron from *Klebsiella variicola*, referred from now on as retron-Kva1 (Mestre-

245   208, clade 1), shows a 10-fold increase editing efficiency compared to Eco1 despite

246   producing only a moderate amount of RT-DNA. Thus, retron-Kva1 represents a particular

247   case that will require further characterization to understand whether another specific

248   feature, such as its predicted non-canonical ncRNA structure, could explain its high

249   recombineering abilities (**Fig 3d**).

250   18 out of the 29 retron candidates were also assessed for their ability to support

251   phage genome recombineering. These retrons were drawn from a subset of high RT-DNA

252   producers across clades, modified to edit phage lambda *xis* gene (stop codon TGA>TAA)

253   using a 70 bp RT-DNA donor. In this case, 4 retrons, including retron-Kva1, show higher

254   recombineering rates than wild-type retron-Eco1 (**Fig 3f**). We found no strong correlation

255   between RT-DNA production and lambda recombineering rates for this set of retrons

256   (**Supplemental Fig 3**); the relative editing of bacterial and phage genomes by individual

257   retrons is only weakly correlated (**Fig 3f**). This could indicate that the biological

258   mechanism of bacterial and phage recombineering differ and that phage biology, RT-DNA

259   structure or additional factors could impact editing rates. However, care should be taken

260   with this interpretation, given that the set of retrons tested for phage editing was selected

261   based on RT-DNA production and genome editing in bacteria.

262

Figure 3. Bacterial editing across retrons. **a.** Schematic of modifications to the retron architecture for encoding a recombineering donor. **b.** Precise editing rate across retrons for bacterial genome recombineering. Points show mean ±SEM. **c.** RT-DNA production versus editing rate (r^2=0.7477, P<0.0001). **d.** Predicted secondary structure of Kva1 ncRNA with sequencing data in orange. **e.** Precise editing rate across retrons for phage genome recombineering. Points show mean ±SEM. **f.** Bacterial versus phage editing rate (r^2=0.2184, P=0.0505). Additional statistical details in **Supplemental Table 2**.

Human precise editing by a diverse set of retrons

To extend the retron census beyond function in bacteria, we tested a diverse set of retrons for their ability to precisely edit the genomes of cultured human cells. Analogous to bacterial and phage editing, a modified RT-DNA encodes an editing donor. In eukaryotic editing, however, this donor is used to precisely repair a genomic site after a targeted double strand break by a Cas9 nuclease. For clarity, we term this combination of a retron with Cas9 for precise editing as an editron.

We synthesized a set of 136 never-before-tested editrons for human editing and four editrons that have been previously tested as internal references. For human editing of the EMX1 locus, a human codon-optimized RT was driven by a constitutive CAG promoter, while a modified ncRNA fused to a CRISPR sgRNA was driven by a Pol III
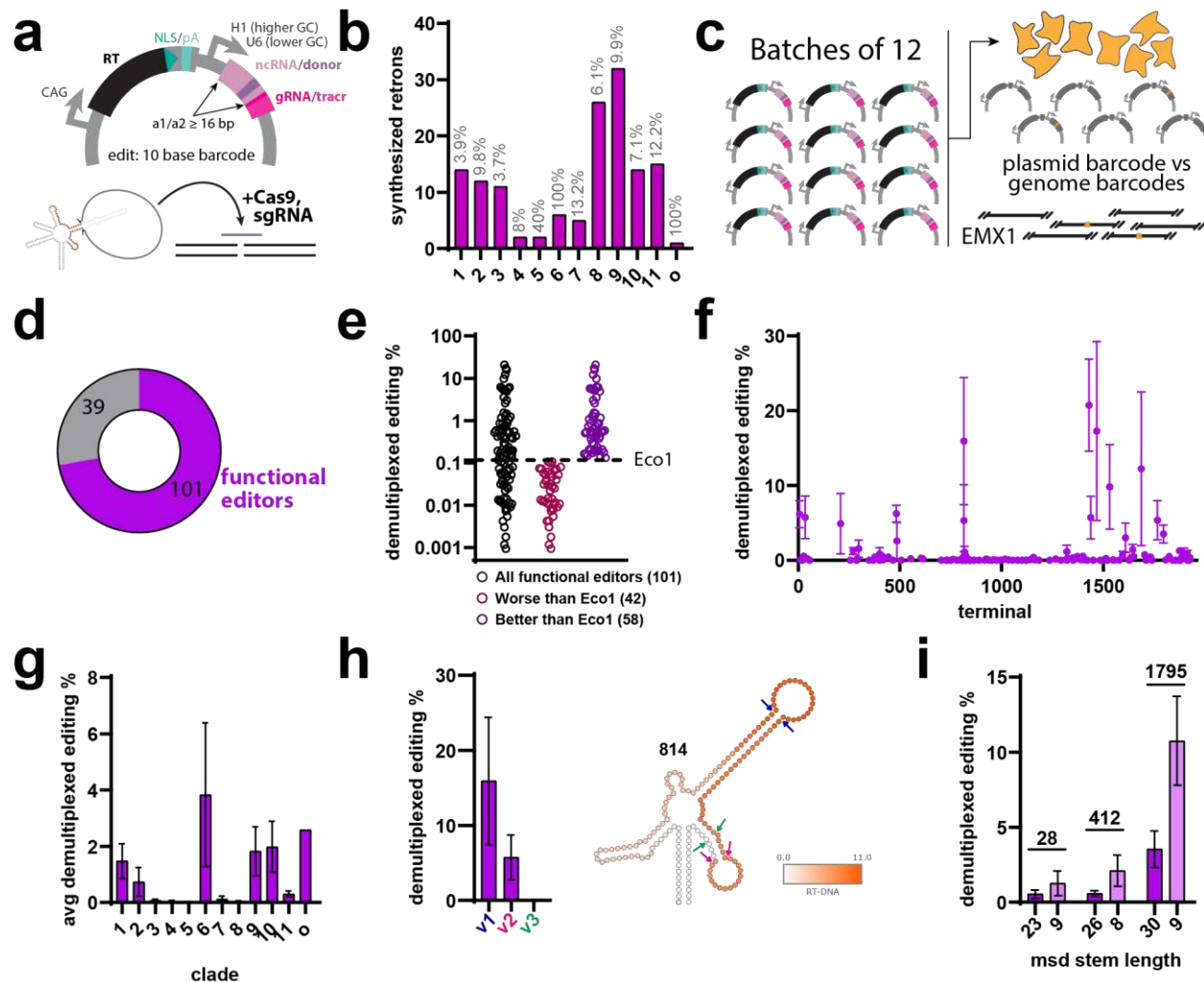
282   promoter (**Fig 4a**). We modified each ncRNA to encode an editing donor in the RT-DNA,

283   which is designed to insert a retron-specific 10 base barcode. The donor also contains a

284   recoding of the PAM nucleotides to protect the ncRNA/sgRNA/RT plasmid and prevent

285   further cutting of the genome after precise editing. Based on previous findings that the

286   length of the retron ncRNA's a1/a2 region can affect editing rates[18], we increased this

287   region of the ncRNA up to 16 bases for any editrons where the endogenous a1/a2 was

288   shorter than 16 bases. We used an H1 promoter to express the ncRNA/sgRNA for most

289   editrons, but used a U6 for a small subset where the H1 promoter was incompatible with

290   synthesis of the retron components. In a parallel experiment, we found that no difference

291   between H1 and U6 promoters for retron-Eco1 (**Supplementary Fig 4a**).

292   As in the bacterial work, we chose the human editrons to sample the phylogenic

293   diversity of retrons, representing each RT clade. Of the 99 total retrons quantified for RT-

294   DNA production and 140 total retrons quantified for human editing, 72 were tested in both

295   conditions. We quantified editing in multiplexed pools of twelve editrons at a time to

296   facilitate testing, using the unique 10 base pair insertion to demultiplex the edits and

297   extrapolate the relative editing rate for each individual member of a pool. Specifically, we

298   quantified the total precise editing rate for a given pool, then assigned a subset of that

299   editing to each member of the pool based on the relative number of barcodes for that

300   retron in the cell genomes and the relative number of plasmids for that retron in the

301   particular pool (**Fig 4c**). Each editron appeared in at least two separate pools to mitigate

302   effects of specific cross-reactivity within a pool.

303   The editron plasmids were transfected into HEK293T cells containing Cas9 pre-

304   integrated into their genomes. Cells were collected three days after transfection. We

305   generated two amplicons per sample for targeted Illumina sequencing: one which

306   amplified the genome (to quantify editing) and one which amplified the plasmid (to

307   account for differences in the relative abundance of retrons plasmids in the pool). We

308   tested retrons in cells with either constitutively expressing or doxycycline inducible

309   versions of the Cas9 and found similar results in both (**Supplemental Fig 4b**), and

310   therefore present a merged dataset.

311   We found that the majority of retrons (101/140) were able to support precise editing

312   to some degree (Fig 4d). Of the functional editrons, we find that 58 of the 101 support

313   higher rates of precise editing than the previous standard retron, retron-Eco1 (**Fig 4e**). As

314   in the case of RT-DNA production, we find that the functional retrons are not randomly

315   distributed across the RT phylogeny, but rather occur in hotspots (**Fig 4f**). In fact, the best

316   editrons were drawn from the same clades (1, 2, 6, 9, 10) as the highest RT-DNA

317   producing retrons (**Fig 4g**). For one retron where we empirically determined the RT-DNA,

318   we tested the placement of the donor at various positions either inside or outside the

319   reverse transcribed region and found, unsurprisingly, that a donor in the core of the RT-

320   DNA had a tendency to support higher levels of editing, consistent with the use of the RT-

321   DNA as the editing donor and not the plasmid itself (**Fig 4h**). Additionally, we tested the

322   effect of donor placement within the RT-DNA stem for three retrons and found that

323   shortening the stem length that flanks the donor yielded higher rates of editing (**Fig 4i**).

324

Figure 4. Human precise editing by a diverse set of retrons. **a.** Schematic of synthesized retron architecture for editing human genomes. **b.** Number of retrons synthesized by clade (percentage of clade synthesized indicated in gray above each bar). Bar o indicates an orphan, clade-less retron. **c.** Schematic of experimental workflow to test retrons in batches of 12. **d.** Proportion of retrons that enable precise editing at any efficiency. **e.** Demultiplexed editing percentage of functional editors, showing a range of efficiencies both above and below the prior reference retron-Eco1. **f.** Demultiplexed editing by retron. Points are mean ±SEM. **g.** Demultiplexed editing by clade (one-way ANOVA, effect of clade, P=0.2197). Bars are mean ±SEM. Bar o indicates an orphan, clade-less retron. **h.** Demultiplexed editing for retron Mestre-814 with the editing donor placed in different stem positions of the msd (one-way ANOVA, effect of donor location, P=0.3774). **i.** Demultiplexed editing for retrons tested with long and short versions of the msd stem (two-way ANOVA, effect of stem length, P=0.0017). Additional statistical details in **Supplemental Table 2**.

DISCUSSION

Retrons are notable for their innate immune function against phages and their applications in biotechnology, particularly for genome engineering. Despite their diversity, prior studies have only explored a limited range of retrons. Herethis study, we conduct a

comprehensive survey of these bacterial systems, focusing on RT-DNA production, bacterial and phage recombineering, and precise human genome editing. This work complements and advances earlier work on retron systems, including an expansion of validated retron RTs, ncRNAs and RT-DNAs. Some of the validated ncRNAs are derived from retron subtypes with no previously predicted ncRNAs (e.g. clade 8, type XI).

The data regarding RT-DNA position within the ncRNA, which can currently only be determined empirically, are particularly valuable. As the number of empirically determined RT-DNA sequences increases, it may become possible to predict future sequences without experimentation. We observed significant variability in RT-DNA production among different retrons, with retrons from certain clades consistently producing more RT-DNA. Another interesting finding is the lack of RT-DNA production in clades 3 and 4. Perhaps the ncRNA from these retrons is noncanonical or positioned far from the retron operon. Alternatively, these retrons may require additional host factors for RT-DNA production.

Our study also sheds light on reverse transcription initiation and termination within retrons. We confirm the presence of a preceding TTA consensus in functional retrons and identify a prevalent AT-rich region at the site of termination area. It is also important to note that some of retrons were visualized as double bands on the gel, and different branched/debranched conformations in sequencing. It has been described that retrons undergo varying maturation processes, which may explain these results[2,25-27].

This research not only provides biological insights but also expands the genome editing toolkit for both prokaryotic and eukaryotic cells. As in previous work[18], we found a strong correlation between RT-DNA production and bacterial editing rates. When editing lambda phage genomes, this correlation was lost. Speculatively, this could be due to anti-

365 retron systems in the lambda genome. Recent work has suggested the presence of an

366 anti-retron protein in phage T5 that reduces the amount of RT-DNA inside the cell[28]. We

367 also show that retron-Kva1 significantly outperforms the previous standard retron-Eco1

368 for both bacterial and phage recombineering, becoming an ideal candidate for further

369 characterization and optimization.

370 We also characterized the ability of phylogenetically diverse retrons to edit

371 mammalian cells, an application which has been limited by a small number of validated

372 retrons. Our work identifies 58 retrons that edit mammalian cells at greater efficiencies

373 than the previous biotechnological standard of retron-Eco1. Interestingly, the top retrons

374 for bacterial RT-DNA production, bacterial recombineering, and human editors are all

375 derived from an overlapping set of RT clades. However, bacterial RT-DNA production is

376 not correlated with human editing at the level of individual retrons (**Supplemental Fig 5**).

377 This difference could reflect RT expression differences in human versus bacterial cells,

378 as well as reverse transcription efficiency. We also demonstrate a new method to test

379 editing of retrons in multiplexed pools which harnesses the unique RT-DNA produced by

380 each retron. This enables a more efficient and trackable screening platform for genome

381 engineering.

382 Overall, our study is the most extensive characterization of retrons to date,

383 validating a larger set of retrons and identifying retrons with better RT-DNA production,

384 bacterial and phage recombineering, and human editing.

385

386 **METHODS**

387 Biological replicates were taken from distinct samples, not the same sample measured

388 repeatedly.

Plapmids

389   **Plasmids**

390   For bacterial expression, retron ncRNA-RT pairs were synthesized into high-copy pET21

391   backbones with T7/lac inducible promoters (Twist). Codons were optimized only if

392   necessary for synthesis. Constructs for recombineering were cloned from these plasmids

393   to add an rpoB editing donor (S512P) or lambda xis editing donor (stop codon TGA to

394   TAA). pORTMAGE-Ec1 was generated previously[29].

395   All human vectors are derivatives of pSCL.273, itself a derivative of pCAGGS[30]. pCAGGS

396   was modified by replacing the MCS and rb_glob_polyA sequence with an IDT gblock

397   containing inverted BbsI restriction sites and a SpCas9 tracrRNA, using Gibson

398   Assembly. The resulting plasmid, pSCL.273, contains an SV40 ori for plasmid

399   maintenance in HEK293T cells. The strong CAG promoter is followed by the BbsI sites

400   and SpCas9 tracrRNA. BbsI-mediated digestion of pSCL.273 yields a backbone for single

401   or library cloning of plasmids with inserts that contain (retron RT - pol III promoter -

402   modified retron ncRNA), by Gibson Assembly or Golden Gate cloning.

403   Retrons for human editing were synthesized into pSCL.273 (Twist). The RT is driven by

404   the CAG promoter. The ncRNA/gRNA cassette was placed under a H1/U6 promoter, with

405   the choice of promoter not impacting editing rates (Supplementary Fig 4a). The donor

406   location loop was determined by viewing RNAFold structures. Typically, the donor was

407   placed at the first unpaired bases of the predicted RT-DNA stem. The reverse transcribed

408   repair template was slightly asymmetric (49 bp of genome site homology upstream of the

409   Cas9 cut site; 71 bp of genome site homology downstream of the cut site) and was

410   complementary to the target strand; in practice, this means that after reverse

411   transcription, the repair template RT-DNA is complementary to the non-target strand, as

412   recommended in previous studies[31]. The repair template for human editing carried three

413   distinct mutations to the EMX1 locus: the first inserts a 10-bp sequence at the Cas9 cut

414   site, with a unique sequence generated for each retron plasmid. The second changes a

415   G>A after the 10-bp insert for the gRNA. The third recodes the Cas9 PAM (NGG → NTT).

416   The gRNA is 20 bp and targets EMX1.

417   Retron accession information as well as all plasmids and ncRNA sequences are listed in

418   **Supplemental Table 1**.

419   **Bacterial Strains and Growth Conditions**

420   The E. coli strains used in this study were DH5α (New England Biolabs) for cloning,

421   bSLS.114[18] for RT-DNA production, bMS.346[15] for bacterial and phage retron

422   recombineering assays. bSLS.114 was constructed from BL21-AI cells using lambda-red

423   replacement to remove the retron-Eco1 locus. bMS.346 was generated from *E. coli*

424   MG1655 by inactivating the *exoI* and *recJ* genes with early stop codons. Bacterial cultures

425   were grown in LB (supplemented with 0.1 mM $MnCl_2$ and 5 mM $MgCl_2$ (MMB) for phage

426   assays), shaking at 37 °C with appropriate inducers and antibiotics. Inducers and

427   antibiotics were used at the following working concentrations: 1mM m-toluic acid (Sigma-

428   Aldrich), 1 mM IPTG (GoldBio), 2 mg/ml L-arabinose (GoldBio), 35 µg/ml kanamycin

429   (GoldBio), and 100 µg/ml carbenicillin (GoldBio).

430

431   **RT-DNA expression and gel analysis.**

432   RT-DNA expression and analysis was performed as previously described[12]. Briefly, retron

433   plasmids were transformed into bSLS.114 for expression. A starter culture from a single

434   clone was grown overnight in 3 ml LB plus antibiotic. After 16h, the culture was diluted

435   (1:100) into 25 ml LB. This culture was allowed to reach OD ~0.5 (approximately 2 hours)

436   and then induced with 1M IPTG and 200 ug/ml l-arabinose. After 5 hours, OD600 was

437   measured and bacteria were harvested for RT-DNA analysis.

438

439   RT-DNA was recovered using a Qiagen Plasmid Plus Midi kit, eluted into a volume of 150

440   ul. Volume RT-DNA prep was adjusted based on bacterial OD, measured at the point of

441   collection, to normalize the input prior to loading into Novex TBE-Urea gels (15%

442   Invitrogen). The gels were run (45 minutes at 200 V) in pre-heated (>75°C) TBE running

443   buffer. Gels were stained with SYBR Gold (ThermoFisher) and then imaged on a Gel Doc

444   Imager (BioRad). To quantify the amount of RT-DNA production relative to retron-Eco1,

445   a retron-Eco1 expressing strain was included every batch of culture grown, and the

446   resulting prep of was always run on the same gel as the experimental retron for

447   quantification. The density of the strongest band of each retron was quantified with

448   ImageJ software.

449

450   **Multiplexed RT-DNA Sequencing**

451   Following Qiagen midipreps, mixes of up to 11 different retrons (including Eco1) were

452   subjected to a DBR1 or sham-DBR1 (water) treatment in the following reaction: 79 ul of

453   RT-DNA prep split evenly depending on the number of retrons in the mix, 10 ul of DBR1

454   (50 ng/uL), 1 ul of RNaseH (NEB), 10 ul rCutSmart Buffer (NEB). The mixes of retrons

455 were organized according to their relative production to retron-Eco1, with the highest

456 producing retrons grouped together and lowest producing retrons grouped together. This

457 minimized the skew in sequencing among the retrons in a pool.

458

459 These reactions were cleaned up with ssDNA/RNA clean & concentrator kit (Zymo

460 Research) and RT-DNA was prepped for sequencing by taking the resulting material and

461 extending the 3′ end in parallel with two types of nucleotides: dCTP or dATP, using

462 terminal deoxynucleotidyl transferase (TdT) (NEB). This reaction was carried out in 1×

463 TdT buffer, with 60 units of TdT and 125 M dATP for 60 s, or 125 M dCTP for 4 minutes

464 at room temperature with the aim of adding ~25 adenosines adenosines or ~6 cytosines

465 before inactivating the TdT at 70°C for 5 min. Next, a primer a polynucleotide, anchored

466 primer was used to create a complementary strand to the   TdT extended products using

467 15 units of Klenow Fragment (3′→5′ exo-) (NEB) in 1× NEB2, 1 mM dNTP and 50 nM of

468 primer containing an Illumina adapter sequence, nine thymines (for the pA extended

469 version) or six guanines (for the pC extended version), and a non-thymine (V) or non-

470 guanine (H) anchor. This product was cleaned up using Qiagen PCR cleanup kit and

471 eluted in 10 ul water. Finally, Illumina adapters were ligated on at the 3′ end of the

472 complementary strand using 1× TA Ligase Master Mix (NEB). All products were indexed

473 and sequenced on an Illumina MiSeq instrument. Previous data from Palka et al. 2022[12]

474 was included in the sequencing analysis for retron-Sen2 (Mestre-116), retron-Eco6

475 (Mestre-488), retron-Eco2 (Mestre-1036), and retron-Eco4 (Mestre-64).

476 **Bacterial Recombineering and Analysis.**

477   To edit bacterial genomes, the different retron cassettes encoded in a pET-21 (+) plasmid

478   and the CspRecT and mutLE32K in the plasmid pORTMAGE-Ec1 were transformed into

479   the bMS.346 strain by electroporation. Experiments were conducted in 500uL cultures in

480   a deep 96-well plate. 3 individual colonies of every retron tested were grown in LB with

481   kanamycin and carbenicillin for 16 h at 37°C. A 1:1000 dilution of these cultures was

482   grown into LB with 1 mM IPTG, 0.2% arabinose and 1 mM m-toluic acid for 16 h with

483   shaking at 37°C. A volume of 25 µl of culture was collected, mixed with 25 µl of water and

484   incubated at 95°C for 10 min. A volume of 1 µl of this boiled culture was used as a

485   template in 25-µl reactions with primers flanking the edit site, which additionally contained

486   adapters for Illumina sequencing preparation. These amplicons were indexed and

487   sequenced on an Illumina MiSeq instrument and processed with custom Python software

488   to quantify the percentage of precisely edited genomes.

489   **Lambda Propagation and Plaque Assays**

490   Lambda was propagated from an ATCC stock (#97538) into a 2mL culture of *E. coli*

491   bMS.346 strain at 37°C at OD600 0.25 in MMB medium until culture collapse. The culture

492   was then centrifuged and the supernatant was filtered to remove bacterial remnants.

493   Lysate titer was determined using the full plate plaque assay method as described by

494   Kropinski et al. 2009[32].

495   **Lambda Recombineering and analysis**

496   The diverse retron cassettes with modified ncRNAs to contain a lambda donor to edit *xis*

497   gene, was co-expressed with CspRecT and mutL E32K from the plasmid pORTMAGE-

498   Ec1. Experiments were conducted in 500uL cultures in a deep 96-well plate. 3 individual

499 cultures were grown for every retron tested for 16h at 37°C. A 1:100 dilution of each

500 culture was induced for 2 h at 37°C. The OD600 of each culture was measured to

501 approximate cell density and cultures were diluted to OD600 0.25. A volume of pre-titered

502 lambda was added to the culture to reach a multiplicity of infection (MOI) of 0.1. The

503 infected culture was grown overnight for 16 h, before being centrifuged for 10 min at 4000

504 rpm to remove the cells. For amplicon-based sequencing, a volume of 25 µl of the medium

505 containing the phage was collected, mixed with 25 µl of water and incubated at 95°C for

506 10 min. A volume of 1 µl of this boiled culture was used as a template in 25-µl reactions

507 with primers flanking the edit site, which additionally contained adapters for Illumina

508 sequencing preparation. Sequencing and editing rates were analyzed as described

509 previously for bacterial recombineering.

510 **Human Editing Pool Design**

511 Editrons were pooled in groups of 12. All editrons appear in at least two different pools

512 (**Supplementary Table 1**). Individual plasmid cultures were started from glycerol stocks

513 in 500 uL of LB Media +Carb for ~6 hours of growth at 37 degrees. Then, OD600 was

514 measured using SpectraMax platereader to determine how much of each culture to add

515 to a mixed culture for equal distribution. Mixed cultures were grown overnight at 37

516 degrees and Midiprepped according to manufacturer's protocol (Qiagen).

517 **Human Cell Culture**

518 For pooled experiments, two Cas9-expressing HEK293T cell lines were used. The first

519 expresses Cas9 from a piggybac integrated, TRE3G driven, doxycycline-inducible (1

520   μg/ml) cassette, which we have previously described[18]. The second expresses Cas9

521   constitutively from a CBh promoter in the AAVS1 Safe Harbor locus (GeneCopoeia

522   #SL502). All HEK cells were cultured in DMEM +GlutaMax supplement (Thermofisher

523   #10566016).

524   T25 cultures were transiently transfected with 12.76 ug of pooled plasmid per T25 using

525   Lipofectamine 3000. Cultures were passaged for an additional 48 h. In the inducible Cas9

526   line, doxycycline was refreshed at passaging. Three days after transfection, cells were

527   collected for sequencing analysis. To prepare samples for sequencing, cell pellets were

528   collected, and gDNA was extracted using a QIAamp DNA mini kit according to the

529   manufacturer's instructions. DNA was eluted in 200 μl of ultra-pure, nuclease-free water.

530   **Human Sample Preparation and Analysis**

531   For pooled samples, 0.5 μl of the gDNA was used as template in 25-μl PCR reactions

532   with primer pairs to amplify the locus of interest and a PCR reaction with primer pairs to

533   amplify the plasmid region, both of which also contained adapters for Illumina sequencing

534   preparation. Lastly, the amplicons were indexed and sequenced on an Illumina MiSeq

535   instrument and processed with custom Python software to quantify the percentage of on-

536   target precise genomic edits normalized to the representation of each plasmid in the pool.

537

538   **Data Availability**

539   All data supporting the findings of this study are available within the article and its

540   supplementary information, or will be made available from the authors upon request.

541 Sequencing data associated with this study is be available on NCBI SRA

542 (PRJNA1047666).

543

Code Availability

545 Custom code to process or analyze data from this study will be made available on GitHub

546 prior to peer-reviewed publication.

547

558

Author Contributions

560 S.C.L, A.G.-D, and S.L.S. conceived the study. M.R.-M. and A.G.-D. performed the

561 experiments in bacteria and phage. A.G.K performed experiments in human cells. S.L.S.,

562 A.G.K., M.R.-M., A.G.-D, S.C.L. and R.F.F. analyzed the data. A.G.K., M.R.-M. A.G.-D,

563 and S.L.S. wrote the manuscript with inputs from all authors.

564

Competing Interests

566 S.L.S. is a founder of Retronix Bio. A.G-D., S.C.L., and S.L.S. are named inventors on

567 patent applications related to the technologies described in this work that are assigned to

568 the Gladstone Institutes and the University of California, San Francisco.
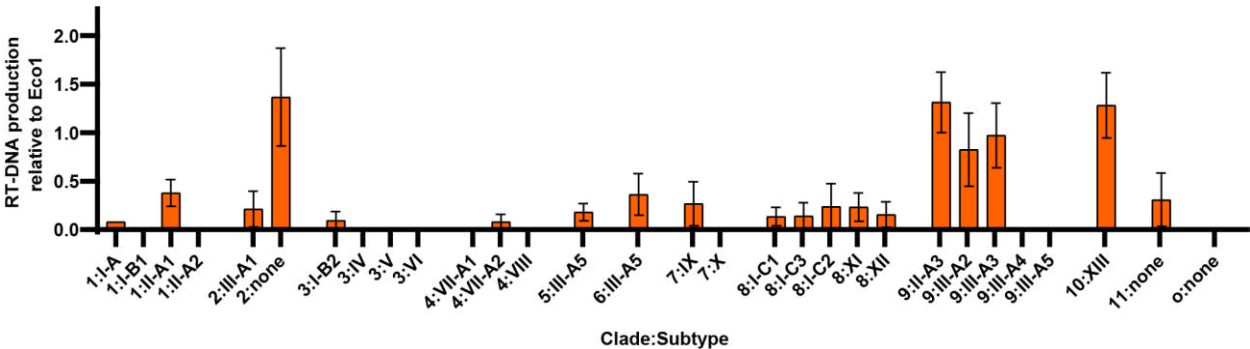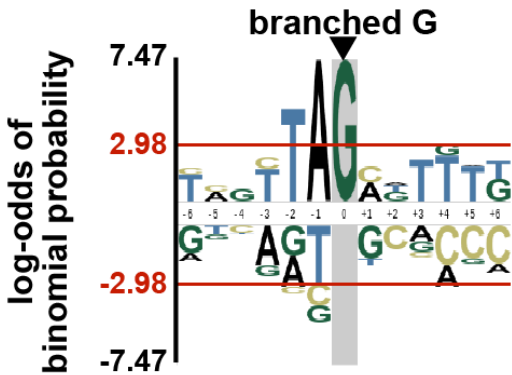
569

CORRESPONDING AUTHOR
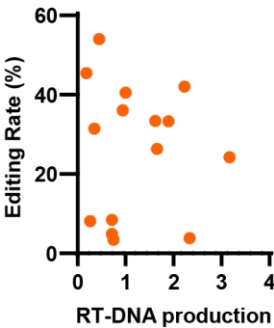
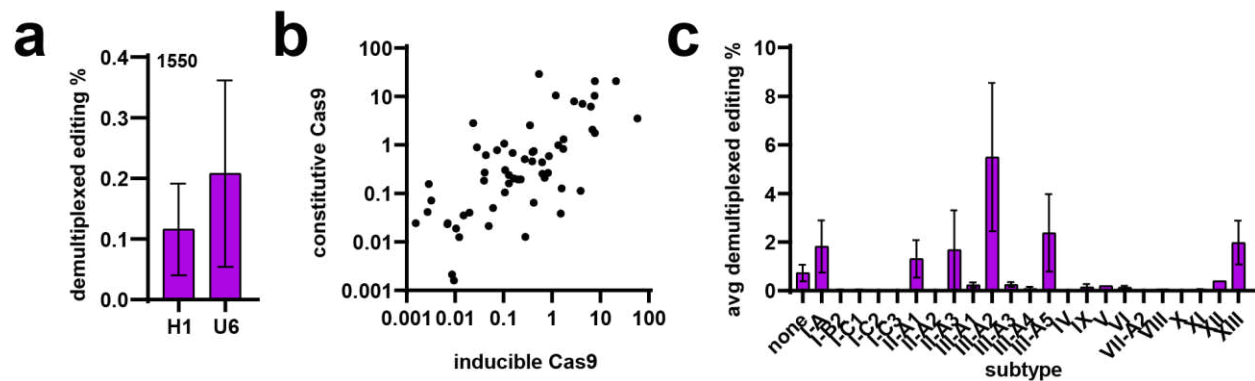571 Correspondence to Seth L. Shipman.

572

Supplementary Figures

Supplementary Figure 1. Related to Figure 1. RT-DNA production relative to Eco1 by clade, separated by subtype. Bars show mean ±SEM.
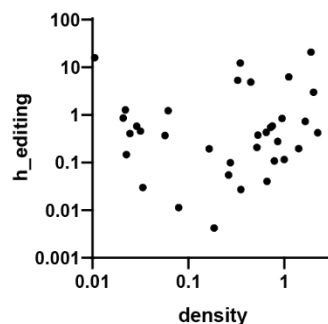

Supplementary Figure 2. Related to Figure 2. Probability logo of ncRNA nucleotides adjacent to the branching guanosine for retrons that produce RT-DNA.

Supplementary Figure 3. Related to Figure 3. RT-DNA production versus with phage lambda recombineering rates (Pearson Correlation (r^2=0.001926, P=0.8766).

Supplementary Figure 4. Related to Figure 4. **a.** Demultiplexed editing percentage by retron-Eco1 (Mestre-1550) comparing the use of an H1 and U6 promoter to drive ncRNA/sgRNA (unpaired T-test, P=0.6256). Bars are mean ±SEM. **b.** Comparison of demultiplexed editing rates of editrons in the constitutive and inducible Cas9 cell lines (Pearson Correlation, r^2=0.4196, P<0.0001). **c.** Average demultiplexed editing rates across retron subtypes. Bars are mean ±SEM.

Supplementary Figure 5. Related to Figure 4. Bacterial RT-DNA production compared with human demultiplexed editing.

References:

1   Yee, T., Furuichi, T., Inouye, S. & Inouye, M. Multicopy single-stranded DNA isolated from a gram-negative bacterium, Myxococcus xanthus. *Cell* **38**, 203-209, doi:10.1016/0092-8674(84)90541-5 (1984). PubMed PMID: 6088065.

2   Inouye, S., Hsu, M. Y., Eagle, S. & Inouye, M. Reverse transcriptase associated with the biosynthesis of the branched RNA-linked msDNA in Myxococcus xanthus. *Cell* **56**, 709-717, doi:10.1016/0092-8674(89)90593-x (1989). PubMed PMID: 2465092.

3   Hsu, M. Y., Eagle, S. G., Inouye, M. & Inouye, S. Cell-free synthesis of the branched RNA-linked msDNA from retron-Ec67 of Escherichia coli. *The Journal of biological chemistry* **267**, 13823-13829 (1992). PubMed PMID: 1378431.

4   Shimamoto, T., Inouye, M. & Inouye, S. The formation of the 2',5'-phosphodiester linkage in the cDNA priming reaction by bacterial reverse transcriptase in a cell-free system. *The Journal of biological chemistry* **270**, 581-588, doi:10.1074/jbc.270.2.581 (1995). PubMed PMID: 7529762.

614   5   Shimamoto, T., Kawanishi, H., Tsuchiya, T., Inouye, S. & Inouye, M. In vitro synthesis
615   of multicopy single-stranded DNA, using separate primer and template RNAs, by
616   Escherichia coli reverse transcriptase. *Journal of bacteriology* **180**, 2999-3002,
617   doi:10.1128/jb.180.11.2999-3002.1998 (1998). PubMed PMID: 9603895; PMCID:
618   PMC107272.
619   6   Simon, A. J., Ellington, A. D. & Finkelstein, I. J. Retrons and their applications in
620   genome engineering. *Nucleic Acids Res* **47**, 11007-11019, doi:10.1093/nar/gkz865
621   (2019).
622   7   Gao, L. *et al.* Diverse enzymatic activities mediate antiviral immunity in prokaryotes.
623   *Science* **369**, 1077-1084, doi:10.1126/science.aba0372 (2020). PubMed PMID:
624   32855333; PMCID: PMC7985843.
625   8   Millman, A. *et al.* Bacterial Retrons Function In Anti-Phage Defense. *Cell* **183**, 1551-
626   1561.e1512, doi:10.1016/j.cell.2020.09.065 (2020).
627   9   Bobonis, J. *et al.* Bacterial retrons encode phage-defending tripartite toxin-antitoxin
628   systems. *Nature* **609**, 144-150, doi:10.1038/s41586-022-05091-4 (2022). PubMed PMID:
629   35850148.
630   10   Mestre, M. R., González-Delgado, A., Gutiérrez-Rus, L. I., Martínez-Abarca, F. & Toro,
631   N. Systematic prediction of genes functionally associated with bacterial retrons and
632   classification of the encoded tripartite systems. *Nucleic Acids Res* **48**, 12632-12647,
633   doi:10.1093/nar/gkaa1149 (2020). PubMed PMID: 33275130; PMCID: PMC7736814.
634   11   Wang, Y. *et al.* Cryo-EM structures of Escherichia coli Ec86 retron complexes reveal
635   architecture and defence mechanism. *Nature microbiology* **7**, 1480-1489,
636   doi:10.1038/s41564-022-01197-7 (2022). PubMed PMID: 35982312.
637   12   Palka, C., Fishman, C. B., Bhattarai-Kline, S., Myers, S. A. & Shipman, S. L. Retron
638   reverse transcriptase termination and phage defense are dependent on host RNase H1.
639   *Nucleic Acids Res* **50**, 3490-3504, doi:10.1093/nar/gkac177 (2022). PubMed PMID:
640   35293583; PMCID: PMC8989520.
641   13   Farzadfard, F. & Lu, T. K. Genomically encoded analog memory with precise in vivo
642   DNA writing in living cell populations. *Science* **346**, 1256272-1256272,
643   doi:10.1126/science.1256272 (2014).
644   14   Sharon, E. *et al.* Functional Genetic Variants Revealed by Massively Parallel Precise
645   Genome Editing. *Cell* **175**, 544-557.e516, doi:10.1016/j.cell.2018.08.057 (2018).
646   15   Bhattarai-Kline, S. *et al.* Recording gene expression order in DNA by CRISPR addition
647   of retron barcodes. *Nature* **608**, 217-225, doi:10.1038/s41586-022-04994-6 (2022).
648   PubMed PMID: 35896746; PMCID: PMC9357182.
649   16   Schubert, M. G. *et al.* High-throughput functional variant screens via in vivo production
650   of single-stranded DNA. *PNAS* **118**, e2018181118, doi:10.1073/pnas.2018181118
651   (2021).
652   17   Lee, G. & Kim, J. Engineered retrons generate genome-independent protein-binding
653   DNA for cellular control. *bioRxiv*, 2023.2009.2027.556556,
654   doi:10.1101/2023.09.27.556556 (2023).
655   18   Lopez, S. C., Crawford, K. D., Lear, S. K., Bhattarai-Kline, S. & Shipman, S. L. Precise
656   genome editing across kingdoms of life using retron-derived DNA. *Nat Chem Biol* **18**,
657   199-206, doi:10.1038/s41589-021-00927-y (2022).

19   Kong, X. *et al.* Precise genome editing without exogenous donor DNA via retron editing system in human cells. *Protein & cell* **12**, 899-902, doi:10.1007/s13238-021-00862-7 (2021). PubMed PMID: 34403072; PMCID: PMC8563936.

20   Zhao, B., Chen, S. A., Lee, J. & Fraser, H. B. Bacterial Retrons Enable Precise Gene Editing in Human Cells. *The CRISPR journal* **5**, 31-39, doi:10.1089/crispr.2021.0065 (2022). PubMed PMID: 35076284; PMCID: PMC8892976.

21   Liu, W. *et al.* Retron-mediated multiplex genome editing and continuous evolution in Escherichia coli. *Nucleic Acids Res* **51**, 8293-8307, doi:10.1093/nar/gkad607 (2023). PubMed PMID: 37471041; PMCID: PMC10450171.

22   Fishman, C. B. *et al.* Continuous Multiplexed Phage Genome Editing Using Recombitrons. *bioRxiv*, 2023.2003.2024.534024, doi:10.1101/2023.03.24.534024 (2023).

23   González-Delgado, A., Lopez, S. C., Rojas-Montero, M., Fishman, C. B. & Shipman, S. L. Simultaneous multi-site editing of individual genomes using retron arrays. *bioRxiv*, doi:10.1101/2023.07.17.549397 (2023). PubMed PMID: 37503029; PMCID: PMC10370050 application related to the technologies described in this work.

24   Mosberg, J. A., Lajoie, M. J. & Church, G. M. Lambda red recombineering in Escherichia coli occurs through a fully single-stranded intermediate. *Genetics* **186**, 791-799, doi:10.1534/genetics.110.120782 (2010). PubMed PMID: 20813883; PMCID: PMC2975298.

25   Lampson, B. C., Inouye, M. & Inouye, S. Retrons, msDNA, and the bacterial genome. *Cytogenet Genome Res* **110**, 491-499, doi:10.1159/000084982 (2005).

26   Kim, K., Jeong, D. & Lim, D. A mutational study of the site-specific cleavage of EC83, a multicopy single-stranded DNA (msDNA): nucleotides at the msDNA stem are important for its cleavage. *Journal of bacteriology* **179**, 6518-6521, doi:10.1128/jb.179.20.6518-6521.1997 (1997). PubMed PMID: 9335306; PMCID: PMC179573.

27   Lease, R. A. & Yee, T. Early events in the synthesis of the multicopy single-stranded DNA-RNA branched copolymer of Myxococcus xanthus. *The Journal of biological chemistry* **266**, 14497-14503 (1991). PubMed PMID: 1713583.

28   Azam, A. H. *et al.* Viruses encode tRNA and anti-retron to evade bacterial immunity. *bioRxiv*, 2023.2003.2015.532788, doi:10.1101/2023.03.15.532788 (2023).

29   Wannier, T. M. *et al.* Improved bacterial recombineering by parallelized protein discovery. *Proceedings of the National Academy of Sciences of the United States of America* **117**, 13689-13698, doi:10.1073/pnas.2001588117 (2020). PubMed PMID: 32467157; PMCID: PMC7306799.

30   Niwa, H., Yamamura, K. & Miyazaki, J. Efficient selection for high-expression transfectants with a novel eukaryotic vector. *Gene* **108**, 193-199, doi:10.1016/0378-1119(91)90434-d (1991). PubMed PMID: 1660837.

31   Richardson, C. D., Ray, G. J., DeWitt, M. A., Curie, G. L. & Corn, J. E. Enhancing homology-directed genome editing by catalytically active and inactive CRISPR-Cas9 using asymmetric donor DNA. *Nature biotechnology* **34**, 339-344, doi:10.1038/nbt.3481 (2016). PubMed PMID: 26789497.

32   Kropinski, A. M., Mazzocco, A., Waddell, T. E., Lingohr, E. & Johnson, R. P. Enumeration of bacteriophages by double agar overlay plaque assay. *Methods in molecular biology (Clifton, N.J.)* **501**, 69-76, doi:10.1007/978-1-60327-164-6_7 (2009). PubMed PMID: 19066811.